



**POLISH ACADEMY OF SCIENCES**

**Systems Research Institute**

**MODELLING CONCEPTS  
AND DECISION SUPPORT  
IN ENVIRONMENTAL SYSTEMS**

**Editors:**

**Jan Studzinski  
Olgierd Hryniewicz**

Polish Academy of Sciences • Systems Research Institute

**Series: SYSTEMS RESEARCH**

**Vol. 45**

---

Series Editor:

**Prof. Jakub Gutenbaum**

Warsaw 2006



**MODELLING CONCEPTS  
AND DECISION SUPPORT  
IN ENVIRONMENTAL SYSTEMS**

**MODELLING CONCEPTS  
AND DECISION SUPPORT  
IN ENVIRONMENTAL SYSTEMS**

Editors:

Jan Studzinski  
Olgierd Hryniewicz

The purpose of the present publication is to popularize information tools and applications of informatics in environmental engineering and environment protection that have been investigated and developed in Poland and Germany for the last few years. The papers published in this book were presented during the workshop organized by the Leibniz-Institute of Freshwater Ecology and Inland Fisheries in Berlin in February 2006. The problems described in the papers concern the mathematical modeling, development and application of computer aided decision making systems in such environmental areas as groundwater and soils, rivers and lakes, water management and regional pollution. The editors of the book hope that it will support the closer research cooperation between Poland and Germany and when this intend succeeds then also next publications of the similar kind will be published.

Papers Reviewers:

Prof. Olgierd Hryniewicz

Prof. Andrzej Straszak

Text Editor: Anna Gostynska

Copyright © Systems Research Institute of Polish Academy of Science,  
Warsaw 2006

Systems Research Institute of Polish Academy of Science  
Newelska 6, PL 01-447 Warsaw

Section of Scientific Information and Publications  
e-mail: biblioteka@ibspan.waw.pl

**ISBN-10: 83-894-7505-7**

**ISBN-13: 978-83-894750-5-3**

**ISSN 0208-8029**

## CHAPTER 2

### **Rivers / Lakes**



## TURBULENCE IN NATURAL STREAMS

Alexander SUKHODOLOV, Tatyana SUKHODOLOVA  
Heinz BUNGARTZ

Leibniz-Institute of Freshwater Ecology and Inland Fisheries, Berlin  
<[alex@igb-berlin.de](mailto:alex@igb-berlin.de); [suhodolova@igb-berlin.de](mailto:suhodolova@igb-berlin.de); [bungartz@igb-berlin.de](mailto:bungartz@igb-berlin.de)>

**Abstract:** River flow represents a valuable factor in fluvial systems and its quantification is crucial for many agricultural, engineering, and ecological aspects of river management. Complete physically sound description of the flow requires knowledge of mean velocity field and turbulent velocity fluctuations. This contribution reports the results of a measurement study exploring structure of turbulence in a lowland river reach. Detailed measurements of turbulence characteristics were made in a representative cross-section of the Spree River using acoustic Doppler velocimeters. Analysis is focused on the spatial distributions of Reynolds stresses and examines the basic mechanisms of Reynolds stresses formation. The study indicates that turbulence on the investigated river reach is dominated by two types of structures – organized motions in the vertical plane and motions coherent in the horizontal plane. It is shown that spatial structure of Reynolds stresses can be reasonably approximated by a simplified analytical model derived from Reynolds equations. A semi-empirical relationship for mean stream wise velocity is proposed. This relation accounts for riverbed and bank friction and therefore expands applicability of conventional logarithmic law.

**Keywords:** river flow, mean velocity, turbulence, Reynolds stresses, measuring system.

### 1. Introduction

River flow represents a valuable factor in fluvial systems and its quantification is crucial for many agricultural, engineering, and ecological aspects of river management. Transport capacities of rivers to deliver solids from the watersheds, sewage from urbanized territories, and capabilities in providing habitats for many species of aquatic life are primarily dependent on the flow velocity fields. Although technical hydrodynamics developed in the last century succeeded to describe velocity fields in simpler cases – for instance in pipes, closed ducts, and smooth channels - our ability to predict velocities in the river flows still hindered because of turbulence.

Conventionally an instantaneous fluid velocity at a point is represented by the sum of a mean value, presumed as being deterministic, and a value of a random character called turbulent fluctuation. Velocity fluctuations and mutual correlations of velocity fluctuations comprise Reynolds stress tensor. The terms of this tensor

demonstrate anisotropic properties in many flows and specifically in rivers. If fluctuations are examined in frequency domain it became evident that anisotropy comes mainly on account of large-scale fluctuations – fluctuations with spatial scales comparable to the dimensions of the flow. Because of ample sizes of water masses experiencing large-scale fluctuations, these masses interact with flow solid boundaries and dependent highly on those interactions specific for certain geometry of the channel. This property of turbulence precludes development of universal theory and hence favors experimental methods.

Experimental studies of turbulence have already long history that rolls back to the pioneering visualization studies of Reynolds (1883). Though first investigations of turbulent structures in canals and rivers were reported almost century ago (Rümelin in 1913), systematic research in field began only in mid-fifties (Yokoshi, 1967; McQuivey, 1973; Grinvald, 1974; Grinvald & Nikora, 1988). Progress in field studies was always hindered by imperfections of measuring devices, logistics of field campaigns, and difficulties in post-processing and interpreting of the data. Recent invention of three-dimensional, high-frequency, remotely sensing acoustic methods have revolutionized the research on river turbulence. During the last decade a growing number of comprehensive studies dedicated to various aspects of turbulent flows in rivers have been reported (Sukhodolov et al., 1998; Nikora & Goring, 2000; Rhoads & Sukhodolov, 2001; Sukhodolov & Rhoads, 2001; Papanicolaou & Hilldale, 2002; Rhoads & Sukhodolov, 2004). Despite the impressive progress such investigations are still limited in their detail mainly on account of laborious logistics of field measurements. Lack of appropriate commercially produced mounting equipment and trained personnel, harsh field conditions of work, high variability of hydraulic flow condition in rivers are still the main limiting factors.

Systematic improvement of field equipment and training for field studies have been performed during last five years in the Department of Ecohydrology, Institute of Freshwater Ecology and Inland Fisheries, Berlin (IGB). As a result of those continuous efforts a set of detailed measurements has been obtained. The purpose of the present paper is to generalize, to a certain extent, the first results of those studies and to outline the directions of further data analysis and interpretation.

## **2. Theory**

Let us consider a coordinate system with streamwise axis  $x$  parallel to the line of mean change in riverbed elevation, transverse axis  $y$  normal to the riverbanks originating at a river centerline (positively directed toward right bank), and vertical axis  $z$  with origin at the mean riverbed elevation and positive direction toward the free surface. The riverbed is inclined at an angle  $\phi$  respect to the horizontal so that its mean slope is  $S \approx \sin \phi$ . The components of velocity vector are denoted as  $u$  for streamwise,  $v$  for transverse, and  $w$  for vertical respectively.

For a steady uniform fully developed turbulent flow in open channel Reynolds equations can be simplified to (Guo & Julien, 2005)

$$\rho v \frac{\partial \bar{u}}{\partial y} + \rho w \frac{\partial \bar{u}}{\partial z} = \rho g S + \frac{\partial \tau_{xy}}{\partial y} + \frac{\partial \tau_{xz}}{\partial z} \quad (1)$$

$$\frac{\partial \bar{v}}{\partial y} + \frac{\partial \bar{w}}{\partial z} = 0 \quad (2)$$

where  $\rho$  is water density,  $g$  is gravity acceleration,  $\tau_{xy} = -\rho \overline{u'v'}$ , and  $\tau_{xz} = -\rho \overline{u'w'}$  are turbulent shear stresses, viscosity of water is neglected. Simple manipulations transform the system (1)-(2) into

$$\frac{\partial \overline{uv}}{\partial y} + \frac{\partial \overline{uw}}{\partial z} = gS - \frac{\partial \overline{u'v'}}{\partial y} - \frac{\partial \overline{u'w'}}{\partial z} \quad (3)$$

or

$$\frac{\partial (\overline{uv} + \overline{u'v'})}{\partial y} + \frac{\partial (\overline{uw} + \overline{u'w'})}{\partial z} = gS \quad (4)$$

where terms in brackets now represent the total shear stresses  $\tau_{xy}$ ,  $\tau_{yz}$  composed of form-induced and turbulent components (Nikora et al., 2001).

Parabolic function was shown to be a good approximate of a river cross-section (Nikora, 1992)

$$z_b = \alpha (2y/B)^\beta \quad (5)$$

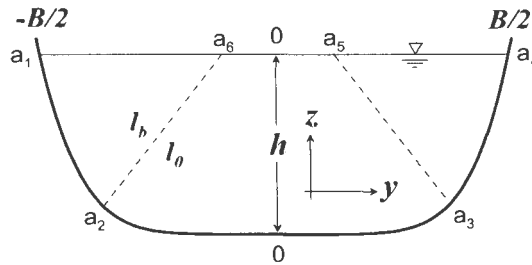


**Figure 1.** Schematic representation of a cross-section.

where  $z_b$  is riverbed elevation,  $B$  is river width, and  $\alpha$ ,  $\beta$  are parameters defined empirically, Figure 1. Laboratory experiments (Tracy, 1965; Guo & Julien, 2005) demonstrate that in proximity of the riverbed the transversal gradients are small as compared to the vertical gradients and the flow area can be divided into three parts:

two near banks  $A_b/2 = A(a_1a_2a_6)$ ,  $A_b/2 = A(a_3a_4a_5)$  and a central  $A_c = A(a_2a_3a_5a_6)$  subsections, Figure 1. Cross-section averaged boundary shear stresses can now be derived integrating equation (4) over the areas  $A_b$  and  $A_c$  (Guo & Julien, 2005)

$$\bar{\tau}_0 = \frac{\rho g S A_c}{L_{2-3}} \quad (6)$$

$$\bar{\tau}_b = \frac{\rho g S A_b}{2H_{1-2}} \quad (7)$$

where  $L_{2-3}$  is distance  $a_3 - a_2$ , and  $H = z(a_2) - z(a_1)$ . Characteristic velocity scales, conventionally called shear velocities, are respectively defined by

$$U_* = \sqrt{\bar{\tau}_0 / \rho} \quad \text{and} \quad (8)$$

$$V_* = \sqrt{\bar{\tau}_b / \rho} \quad (9)$$

From (6) and (7), assuming that in rivers the width to depth ratios are normally large, and  $A_c > A_b$ , one obtains a relationship for shear velocities  $U_* \geq V_*$ .

Considering flow in the central part of hydraulically rough channel and neglecting horizontal component of the Reynolds stresses tensor after integration over the local flow depth  $h$  and accepting zero boundary condition at the flow surface, yields

$$\tau_{XZ} = \rho g S h (1 - z/h) = -\overline{u'w'} - \overline{u\bar{w}} \quad (10)$$

where  $z = z - z_b$  is distance from the riverbed. Equation (10) allows further subdivision of the flow in hydraulically rough channels into two sublayers: form induced sublayer where turbulent stresses are relatively small and the outer sublayer where form-induced terms  $\overline{u\bar{w}}$  are small in comparison with turbulent (Nikora et al., 2001). Accordingly, in the outer sublayer equation (10) reduces to

$$\tau_{XZ} \approx \tau_{xz} = \rho g S h (1 - z/h) = -\overline{u'w'} \quad (11)$$

and a local characteristic velocity scale or shear velocity is defined  $u_* = \sqrt{\tau_0 / \rho}$ ,  $\tau_0 = \rho g h S$ . Note that near the banks equation (4) should be integrated only over a portion of the local depth from  $z_b$  to  $z = z_b + l_0$  and  $u_* = \sqrt{g l_0 S}$  respectively.

Similarly integrating equation (4) for the area near the banks, neglecting vertical components of the Reynolds stresses at a certain elevation  $z$  and implying zero boundary condition for horizontal shear stress at the central part of the cross-section, one obtains

$$\tau_{xy} = \rho g S l_b (1 - y/b) = -\overline{u'v'} - \overline{u} \overline{v} \quad (12)$$

where  $y = -y - B/2$ ,  $b = l_b = (b_c - B)/2$  for negative  $y$ , and  $y = y - B/2$ ,  $b = l_b = (B - b_c)/2$  for positive  $y$  values. Expanding the multilayer model of turbulent flow in hydraulically rough open-channel (Nikora et al., 2001) to the case of three dimensional flow, yields

$$\tau_{xy} \approx \tau_{xy} = \rho g S l_b (1 - y/b) = -\overline{u'v'} \quad (13)$$

Equation (13) defines then a local transversal shear velocity  $v_* = \sqrt{\tau_b / \rho}$ ,  $\tau_b = \rho g l_b S$ .

Equations (5), (10)-(13) represent a simple analytical model of the flow in natural streams. This model can be used, for example, to compute mean velocity field if a closure scheme relating Reynolds stresses to mean velocity is provided. Particularly application of Boussinesq hypothesis leads to logarithmic distribution of mean velocities. However, apart of importance of those equations for modeling purposes, they represent convenient analytical framework for analysis and interpretation of turbulence field measurements.

### 3. Field measurements

**River reach** A measurement study was performed in the lowland river Spree near the village Freienbrink, 10 km east of Berlin, Germany. In the study reach the channel is straight with stone armored banks and with a bed covered by sands of about 1 mm in diameter. Measurements were performed during 2 – 6 June 2003 at water discharge of 4.9 m<sup>3</sup>/s that provided following bulk characteristics of the flow: mean velocity 0.27 cm/s, river width 20.45 m, averaged depth 0.89 m, free surface slope  $4.65 \times 10^{-5}$ , Froude number 0.09, Reynolds number  $2.18 \times 10^5$ , shear velocity 2.0 cm/s.

**Measuring systems** The acoustic Doppler velocimeter (ADV) was used to measure velocities in this study. The device is capable of remotely sensed three-component sampling velocities at high frequency of sampling - 25Hz and higher with new models (Micro-ADV, Vectrino).

To mount ADV probes customary manufactured mounting equipment was employed in this study. This equipment consists of an adjustable light weight bridge for applications in river with a maximum depth of 2 meters, Figure 2. The bridge was designed for accurate positioning and easy traversing of the devices across and spanwise the flow, and to prevent flow-induced vibration of the instruments. Alignment of ADV probes and determination of water slopes were performed with a laser total station Elta R55. Local river depth was measured with standard hydrometrical

wading rods. River bed material was collected manually with a simple handy sampler.

**Measurement program** Measurements were performed in a cross-section of the river at vertical profiles positioned at approximately 1 m intervals across the river. These profiles consisted of 12 measuring points each evenly distributed over the local river depth. Intervals between measuring points varied from 3 to 9 cm depending on the local depth at the vertical. Velocities were sampled at 25 Hz during 4 minutes periods. Prior to and after velocity measurements at every profile, water slope for entire river reach was measured at three water level gauges located upstream, in the middle and downstream sections of the reach.



Figure 2. Mounting bridge with leveling nodes.

**Data processing** Time series of velocity measurements were processed with a versatile commercial software package ExploreV 1.5, Nortek AS, Norway. The software provides interactive graphical environment enabling fast and comprehensive data treatment. It allows editing, clipping, filtering of row data, stationarity, spectral, cross-spectral and other advanced methods of analysis including the data processing on a spatial grid.

With the use of ExploreV measured time series were inspected visually to identify possible problems, such as spikes, trends or abrupt discontinuities in the time series. Frequency distributions of the velocity data were also examined to identify outliers. Examination of these distributions is especially valuable for determining errors associated with large spikes resulting from interruption of the acoustic signal by large pieces of debris moving through the sampling volume. Spikes always generated velocity values more than 3 standard deviations from the mean ( $3\sigma$ ).

These spikes were removed and replaced with values generated by linear interpolation between adjacent data using a  $3\sigma$  filter in the time series option of ExploreV. In all cases this post-processing procedure did not greatly affect the values of means, producing changes of only few mm/s.

#### 4. Results and Analysis

**Riverbed morphology** Riverbed morphology for the experimental reach is presented in Figure 3. The map of riverbed elevations indicates that the dominant morphological structures on the river reach are represented by wave-like alternating structures about two times of river widths in lengths and about 25 cm high. Although these morphological structures resemble certain similarity with classical alternate bars, they are too small in their height and relatively short in the streamwise extent in comparison with alternate bars normally observed in rivers (Kondratiev et al., 1982). However, besides the dimensions, the observed bedforms differed from the classical alternate bars by their migration rates. Observed bedforms were stable and practically immobile.

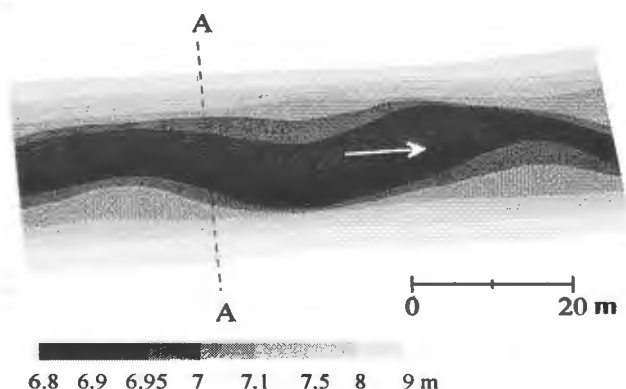


Figure 3. Morphology of the Spree River reach near Freienbrink, contours indicate elevations on arbitrary datum.

**Mean Velocities** Mean streamwise velocity distribution in the cross-section A-A is shown in Figure 4. Mean velocity pattern resembles a typically observed distribution in the open-channel flows. Velocity magnitude increases gently from the riverbed toward the surface and from the banks toward the centerline. Although there are some deviations from the symmetry, considering variability of riverbed morphology in general, this pattern could be perceived as a symmetrical. Mean transversal velocities varied within  $\pm 1.5$  cm/s about zero everywhere in the cross-section A-A and therefore are not shown here. Velocity deep phenomenon indicating significant effect of secondary currents is not pronounced in the pattern of streamwise velocities.

**Reynolds stresses** Distribution of Reynolds stresses components in the cross-section A-A is shown in Figure 5. Pattern of  $-\overline{u'w'}$  component shown in Figure 5a meets general expectations - maximal values are observed near the riverbed in the central part of the cross-section and the stresses reduce to zero near the free surface. Reduction of  $-\overline{u'w'}$  is also observed near the banks. There is a small spot near the right bank where  $-\overline{u'w'}$  changed the sign - an effect that might be characteristic for secondary currents. Another distinctive feature of the pattern is its non-uniformity.

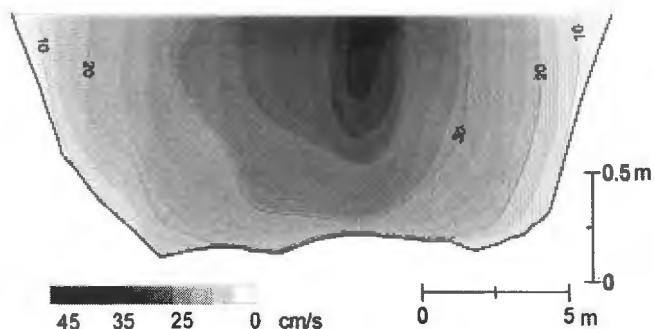


Figure 4. Mean velocity distributions in the cross-section A-A (isovels are in cm/s).

Relief of  $-\overline{u'w'} = f(y, z)$  indicates a presence of the local peaks separated by valleys of reduced values.

Reynolds stress component  $-\overline{u'v'}$  is presented in Figure 5b. As expected from theoretical considerations, and in accordance with previous laboratory investigations, the maximum values of  $-\overline{u'v'}$  are mainly observed near the free-surface of the flow. Unexpectedly high values can be also seen near the riverbed on the right side of the channel. Function  $-\overline{u'v'} = f(y, z)$  changes its sign in the central part of the flow and the parts of the section with opposing signs are demarcated with practically vertical interfacing line ( $-\overline{u'v'} = 0$ ).

Valuable information about spatial structure of Reynolds stresses and their local dominancy could be comprehended from the spatial distribution of ratio between components of the stress tensor, particularly  $|\overline{u'v'}|/|\overline{u'w'}|$  (Figure 5c). Spatial distribution in Figure 5c clearly indicates that flow is dominated by vertical components of the stress  $-\overline{u'w'}$  in the range of dimensionless distances from the bed  $0 < z/h < 0.75$ . Upper, pre-surface layer of the flow ( $0.75 < z/h < 1.0$ ) is strongly dominated by horizontal component of the stress  $-\overline{u'v'}$ . However, there exist some small areas near the riverbed where horizontal stresses are comparable or even larger than  $-\overline{u'w'}$ . Reynolds stress component  $-\overline{v'w'}$  was very small in comparison with

two other components everywhere in the cross-section A-A and therefore is not received consideration here.

**Scaling Reynolds Stresses** According to equation (10), the distribution of Reynolds stresses component  $-\overline{u'w'}$  should scale on shear velocity  $u_*$ . For an individual profile particulate value of shear velocity can be determined fitting linear regression to a measured distribution  $-\overline{u'w'}$  in the outer sub-layer of the flow (Nikora et al., 2001) satisfying condition (11).

Measured  $-\overline{u'w'}$  vertical profiles were normalized by fitted shear velocity values and plotted in Figure 6. The data set was subdivided into four sub-sets. Each sub-set corresponds to a certain range of relative distances  $-0.5 < y/b < 0.5$ ,  $b = B/2$  from the centerline of the channel. For example, distribution of normalized Reynolds stresses for the central part  $-0.15 < y/b < 0.15$  is shown in Figure 6a. Equation (11) is represented in this plot by solid line and dashed lines indicate 5% accuracy intervals. Gray scales outline the ranges of form induced and interfacial sub-ranges. The upper boundary of the form-induced sub-range was determined as the distance from the river bottom at which measured normalized stresses deviated significantly from 5% accuracy interval. Analysis of vertical distributions indicates that most closely (scatter within  $\pm 5\%$ ) measured values follow theoretical description, equation (11), in the central part  $-0.15 < y/b < 0.15$  for dimensionless distances ranging from  $0.3z/h$  to  $1.0z/h$ . Scatter in the data remains moderate, within  $\pm 10\%$  interval, as the locations approach the banks ( $-0.35 < y/b < -0.15$  and  $0.15 > y/b > 0.35$ ), though the height of the form induced sub-layer is slightly increasing (Figure 6b). Near the corners of the channel stresses profiles indicate very distinctive pattern (Figure 6c). They characterized by pronounced increase of positive contribution of turbulence that has to be offset by negative contribution of mean velocity correlation in accordance with equation (10).

Shear velocity values obtained from individual Reynolds stresses vertical profiles (Figure 6) can be scaled with values computed from relationships (6)-(9). However, in many practical situations, when the areas of bank influence is not known in advance, equations (6) and (8) used, and the averaged shear velocity is simply defined as  $U_* = \sqrt{gHS}$  where  $H$  is mean depth on the river reach.

a)

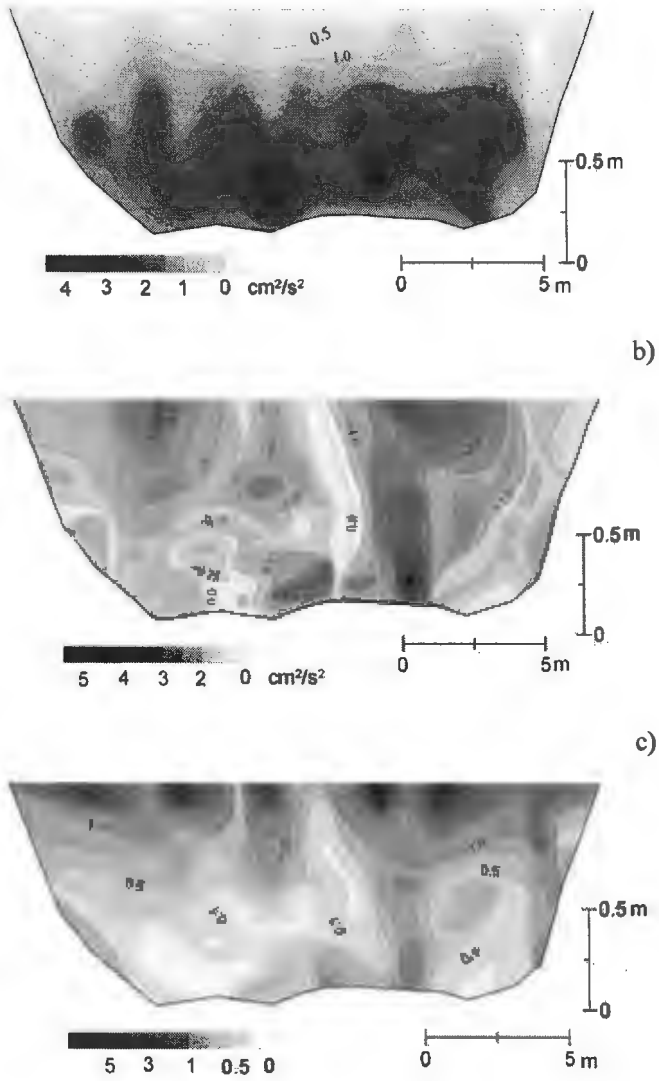


Figure 5. Distribution of Reynolds stresses  $-\overline{u'w'}$  (a),  $-\overline{u'v'}$  (b), and ratio  $|\overline{u'v'}|/|\overline{u'w'}|$  (c) in the cross-section A-A.

a)

b)

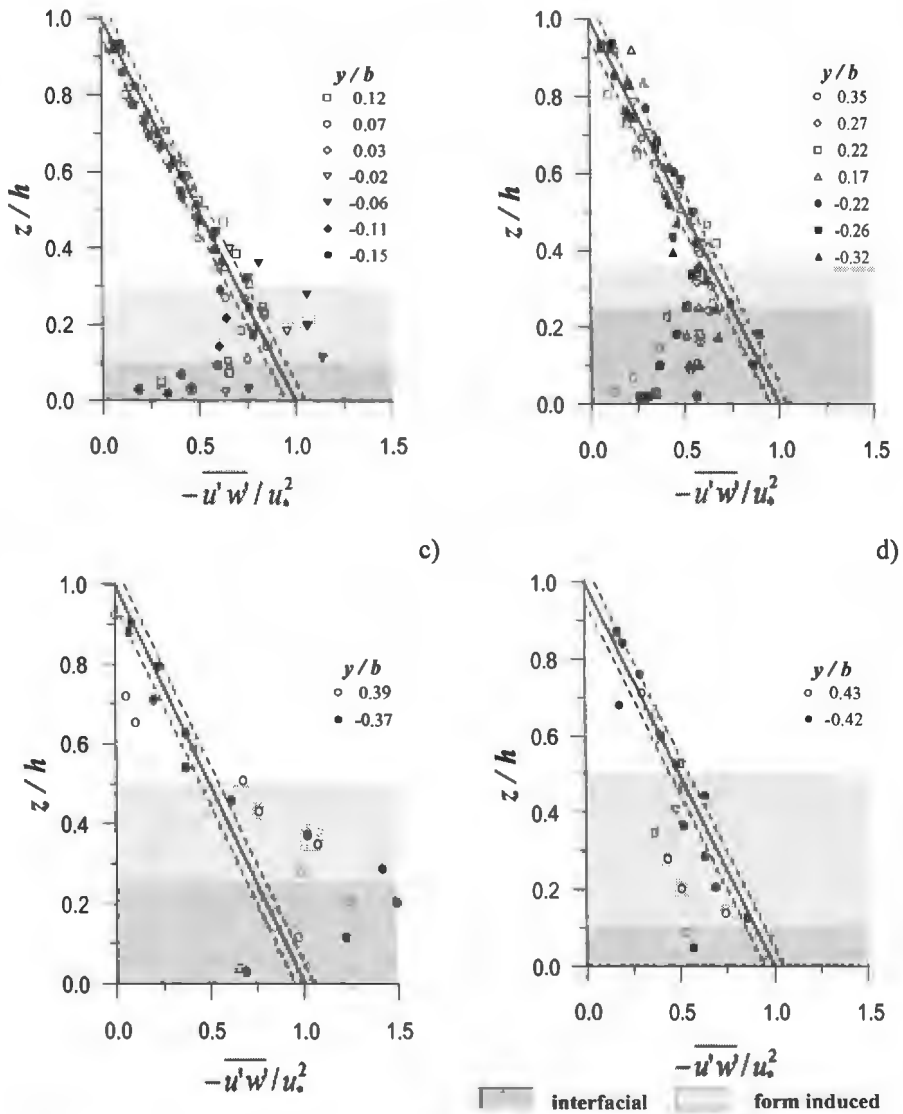
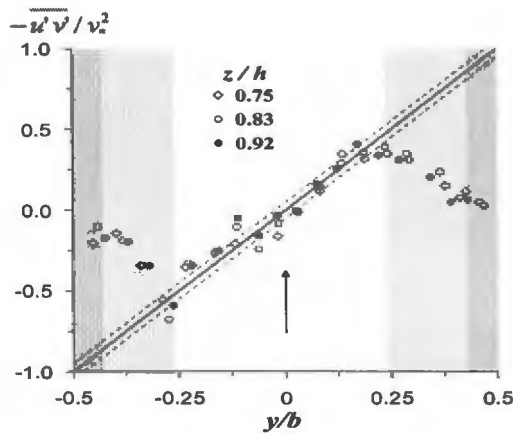


Figure 6. Vertical distribution of Reynolds stresses.

Because equations (10)-(11) are shown to perform reasonable well over substantial area of the flow the local shear velocities can be also defined as  $u_* = \sqrt{g h S}$ . Using this simplified equation together with relationship (5) which defines the local river depth as  $h = z_s - z_b$ , where  $z_s$  is the elevation of the flow free surface.



**Figure 8.** Horizontal distribution of normalized Reynolds stresses

Now we are able to compare normalized measured shear stresses  $\tau'_m = u_* (y/b)/U_*$  to normalized predicted shear stresses  $\tau'_p = \sqrt{h(y/b)/H}$ , Figure 7. Noteworthy is that equation (5) perfectly matches spatially averaged cross-sectional profile of the river reach. Averaging was performed on an ensemble of three hundred cross-sectional profiles extracted from a digital model of the river channel. Obtained data indicate general agreement with simple predictions based on solution for uniform open-channel flow. Accuracy of prediction is within  $\pm 15\%$  intervals indicated by dashed lines in Figure 7.

In the horizontal plane scaling of transverse component of Reynolds stresses  $-\overline{u'v'}$  can be performed with the use of equation (13). To obtain the value for scaling parameter  $v_*$  measured distributions of  $-\overline{u'v'}$  at several depth horizons were linearly fitted in accordance with (13). Obtained values of shear velocity  $v_*$  for left hand side of the river ( $-0.5 < y/b < 0$ ) ranged from 1.8 to 2.2 cm/s, and for right hand side ( $0 < y/b < 0.5$ ) they ranged from 2.8 to 3.4 cm/s. These values closely agree with estimates obtained from  $U_* = \sqrt{gHS}$  suggesting that  $V_* \approx U_*$ . Normalized Reynolds stress components  $-\overline{u'v'}/v_*^2$  are shown in Figure 8.

Close grouping of measured data indicates an agreement with equation (13) in the range  $-0.25 < y/b < 0.25$ . Similarly to prediction of reach-averaged shear velocities  $U_*$  from  $U_* = \sqrt{gHS}$ , one could expect that, according to (9), reach-averaged shear velocity can be obtained from  $V_* = \sqrt{gbS/2}$ . For the investigated river reach this relationship yielded value about 4.0 cm/s. An error (about 30%) in

the estimate accounts for a crude representation of the area of influence of the bank shear in a triangle shape. Measurements, Figure 8, indicate that the area of influence of bank shear is even smaller. Nevertheless the crude estimate is still good and can be used in practical applications.

**Application for flow modelling** From similarity consideration or applying mixing length hypothesis one obtains a logarithmic law describing velocity distribution over river depth. Particular form of the logarithmic function is velocity defect law

$$\frac{\bar{u}_0 - \bar{u}(z)}{u_*} = \frac{1}{\kappa} \ln \frac{z}{h} \quad (14)$$

Velocity defect law (14) assumes quasi-two-dimensional channel flow which is approximately established in the central part  $y \approx 0$  of the river. To expand the applicability of (14) to the whole cross-section requires specification of its parameters  $u_*$  and  $\bar{u}_0$  as functions of transverse coordinate  $y$ .

As it was already demonstrated in the section 3.4, the transversal distribution of bottom shear stresses can be predicted using the local depths values. With a simple algebra by virtue of (5) one obtains

$$u_*(y) = \hat{u}_* \left( 1 - (2y/B)^\beta \right)^{1/2} \quad (15)$$

where  $\hat{u}_* = u_*(y=0)$ . Distribution of mean velocity in the outer layer of the flow can be represented by a power function

$$\frac{\bar{u}_0}{u_0} = \left( 1 - \frac{2y}{B} \right)^m \quad (16)$$

where  $m$  is an empirical parameter. Substituting (15) and (16) into (14) yields

$$\frac{\bar{u}(y, z)}{u_*(y)} = \frac{1}{\kappa} \ln \frac{h}{z} + C_f \frac{(1 - 2y/B)^m}{(1 - (2y/B)^\beta)^{1/2}} \quad (17)$$

where  $C_f = \hat{u}_0 / \hat{u}_*$  is friction coefficient at  $y=0$ . The value of friction coefficient can be determined with the use of a semi-empirical relationship (Sukhodolov et al., 1998)

$$C_f = 2.5 \ln \frac{h}{a(\hat{u}_*^2/g)^n} \quad (18)$$

where  $a = 7.99 \times 10^3$  and  $n = 2.71$ . Relationship (18) was established from a comprehensive set of field and laboratory data and has been shown to predict with accuracy about 20%. The value of the parameter  $m$  was determined from the distribution of mean velocities (Figure 4) and equaled 0.37.

The performance of the model (5), (17), and (18) was tested on a data set of hydrometric surveys conducted in the Spree River at Freienbrink during 1993-1995. Velocities in this surveys were collected with electromagnetic current meter taking 5 point measurements over verticals spanning the cross-section by 2 meter intervals. The measured data, their best fit approximation and computations with the model are shown in Figure 9. Overall good predictive capabilities of the model can be conjectured from these plots.

## 5. Discussion and Conclusions

This study explores the structural properties of the turbulent flow in a straight reach of the lowland river Spree. Detailed measurements of turbulence characteristics were completed with the use of state-of-the art acoustic Doppler velocimeters. Analysis of obtained data is focused on spatial distributions of Reynolds stresses – the most valuable turbulence quantities. Obtained data compared to the analytical models and comparison revealed in most cases an agreement with simplified theoretical predictions.

Theoretical deduction provided a set of algebraic relationships for spatial distribution of Reynolds stress components  $\overline{u'w'}$ , and  $\overline{u'v'}$ , equations (11) and (12). These relationships were obtained with the assumption on dominance of one component on another over the certain area of the flow. Detailed measurements completed in the experimental river reach in general revealed the applicability of this assumption and allow outlining approximate boundaries for flow parts. This scheme shows that, except a small area near the bottom, the spatial distribution of Reynolds stresses can be described by a simplified analytical model (11)-(12). The area near the river bed marked as “bed-form-induced horizontal structures” is related to the effect of riverbed morphology. This structure obviously develops at the trough of a bedform located upstream the section A-A, Figure 3. Unfortunately at the moment there is no appropriate theoretical approach to describe the effect of meso-scale morphological structures on flow structure.

Reynolds stress distributions in vertical plane can be accurately scaled with bulk shear velocity for the central part of the flow  $-0.3 \leq y/b \leq 0.3$  for the range of dimensionless distance from riverbed  $0.3 \leq z/h \leq 1.0$ , Figures 6. There was also observed growths of the form-induced layer thickness from the center of the flow toward riverbanks. Thickness of form-induced layer was maximal at bank corners - that indicates that the effect most probably comes from the shape of the channel. To summarize the issue on Reynolds stresses, it should be concluded that distribution of Reynolds stresses in natural streams is a complex and contributed by different factors: friction over the riverbed and banks, effect of bedforms and the channel shape. Simplified theoretical approaches provide reasonable description of Reynolds stresses for the central part of the flow. The accuracy of prediction is within  $\pm 20\%$ . Near solid boundaries of the flow the deviations are much greater and the appropriate description in many cases lacking. This situation is common for different

branches of fluid mechanics and hydrodynamics of turbulent flows. Even in simple cases of flow over smooth surfaces treatment of flow near boundaries require application of special, sometimes purely empirical, functions.

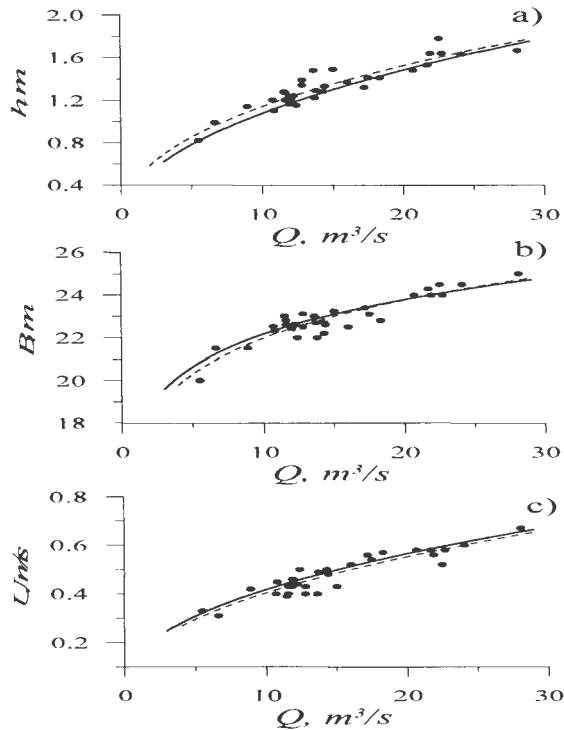


**Figure 9.** Measured and predicted bulk characteristics of the flow.

Further development of river flow hydrodynamics will obviously require elaboration of special formulations describing structure of the flow near boundaries. This is also important that future studies should consider specific types of bedforms, and first of all meso-forms, on the riverbed.

### Acknowledgements

Christof Engelhardt and Nicholas Nikolaevich are thanked for their assistance with field surveys. The research was supported in parts by Deutsche Forschungsgemeinschaft (SU 405/2-1, BU 1442/1-1) and by Collaborative Programme of NATO (ESP.NR.EV 981608).

### References

- Grinvald D.I. (1974) *Turbulence of River Flows*. Leningrad: Hydrometeoizdat.  
 Grinvald D.I., Nikora V.I. (1988) *River Turbulence*. Leningrad: Hydrometeoizdat.

- Guo J., Julien P.Y. (2005) Shear stress in smooth rectangular open-channel flows. *Journal of Hydraulic Eng.* ASCE, **131**(1): 30-37.
- Kondratiev N.E., Popov I.V., Snishenko B.F. (1982) *Foundations of Hydromorphological Theory in Channel Processes*. Leningrad: Hydrometeoizdat.
- McQuivey R.S. (1973) Summary of turbulence data from rivers, conveyance channels and laboratory flumes. *USGS Prof. Paper* 802-B.
- Nikora V.I. (1992) *Channel Processes and Hydraulics of Small Rivers*. Kishinev: Stiinza.
- Nikora V.I., Goring D.G. (2000) Flow turbulence over fixed and weakly mobile gravel beds. *Journal of Hydraulic Eng.* ASCE, **126**(9): 679-690.
- Nikora V., Goring D., McEwan I., Griffiths G. (2001) Spatially averaged open-channel flow over rough bed. *Journal of Hydraulic Eng.* ASCE, **127**(2): 123-133.
- Papanicolaou A.N., Hilldale R. (2002) Turbulence characteristics in gradual channel transition. *Journal of Emg. Mech.*, **128**(9): 948-960.
- Reynolds O. (1883). An experimental investigation of the circumstances which determine whether the motion of water shall be direct or sinuous, and the law of resistance in parallel channels. *Philos. Trans. R. Soc. London Ser.A* 174: 935-982.
- Rhoads B.L., Sukhodolov A. (2001) Field investigation of three-dimensional flow structure at stream confluences: Part I. Thermal mixing and time-averaged velocities, *Water Res. Res.* AGU, **37**(9): 2393-2410.
- Rhoads B.L., Sukhodolov A. (2004) Spatial and temporal structure of shear-layer turbulence at a stream confluence. *Water Res. Res.* AGU, **40**(6): W06304 10.1029/2003WR002811.
- Rümelin Th. (1913) *Wie bewegt sich fließendes Wasser?* Dresden: Zahn & Jaensch.
- Sukhodolov A., Thiele M., Bungartz H. (1998) Turbulence structure in a river reach with sand bed, *Water Res. Res.*, **34**(5): 1317-1334.
- Sukhodolov A., Rhoads B.L. (2001) Field investigation of three-dimensional flow structure at stream confluences: Part II. Turbulence, *Water Res. Res.*, AGU, **37**(9): 11-2424.
- Tracy H.J. (1965) ent flow in a three-dimensional channel. *Journal Hydraulic Div.* ASCE, **91**(9): 9-35.
- Yokoshi S. (1967) The structure of river turbulence. *Bul. Dis. Prev. Res.*, 17: 1-29.

**Jan Studzinski, Olgierd Hryniewicz (Editors)**

**MODELLING CONCEPTS AND DECISION  
SUPPORT IN ENVIRONMENTAL SYSTEMS**

This book presents the papers that describe the most interesting results of the research that have been obtained during the last few years in the area of environmental engineering and environment protection at the Systems Research Institute of the Polish Academy of Sciences in Warsaw and the Leibniz-Institute of Freshwater Ecology and Inland Fisheries in Berlin (IGB). The papers were presented during the First Joint Workshop organized at the IGB in February 2006. They deal with mathematical modeling, development and application of computer aided decision making systems in the areas of the environmental engineering concerning groundwater and soil, rivers and lakes, water management and regional pollution.

**ISBN-10: 83-894-7505-7**

**ISBN-13: 978-83-894750-5-3**

**ISSN 0208-8029**

---

---